Recent advances in helioseismic predictors of space weather

F. Hill

National Solar Observatory, Tucson, AZ, USA

Abstract. Helioseismology probes the solar interior using acoustic oscillations. With current and future experiments providing continuous data that can be analyzed via local helioseismology techniques, there is now the potential of using subsurface observations to predict space weather. Several relevant developments in helioseismology are reviewed here. These include holographic imaging of the farside of the sun; time-distance studies of rising active regions; and ring diagram analysis of twisting flows underneath strongly-flaring active regions.

Index Terms. Helioseismology, solar activity, space weather.

_____

1. Introduction

Helioseismology is a very effective tool for probing the solar interior. The properties of acoustic oscillations trapped in the internal solar temperature gradient are determined by the characteristics of the plasma through which the waves travel. Thus, precise measurements of the wave properties (e. g. frequency, amplitude, phase, etc.) can be used to infer the physical conditions (e.g. flow velocity, sound speed) below the photosphere.

With the advent of modern helioseismology observational assets, such as the space-based Michelson Doppler Imager (MDI) on the Solar and Heliospheric Observatory (SOHO) and the ground-based Global Oscillation Network Group (GONG) program, our knowledge of the solar interior has dramatically improved. In the future, the Solar Dynamics Observatory (SDO) mission will provide another quantum leap in our understanding, thanks to the Helioseismic and Magnetic Imager (HMI) instrument.

This paper reviews some recent advances in helioseismology that could provide predictors of space weather. These include holographic imaging of the farside of the sun; time-distance studies of rising active regions; and ring diagram analysis of twisting flows underneath strongly-flaring active regions.

2. Global helioseismology and the solar cycle

Helioseismology analysis comprises two areas distinguished by the spatial scales of the phenomena that are probed and the representation of the waves. Global (as contrasted with local) helioseismology analyzes the normal modes of the sun as a whole. The oscillations are treated as spherical harmonics, and the resulting inferences are averaged over the entire sun. Thus, the results are functions of depth and latitude only, and symmetric across the equator.

This type of analysis has provided several useful results. An example is seen in Fig. 1, which shows the residual zonal flow at a depth of 0.7 Mm as a function of date and latitude. The pattern of the torsional oscillation is clearly evident. Further analysis indicates that the torsional oscillation signature extends down to the middle of the convection zone (Howe et al., 2005). This suggests that the origin of the torsional oscillation is at the base of the convection zone, rather than at the surface as suggested by Spruit (2003).
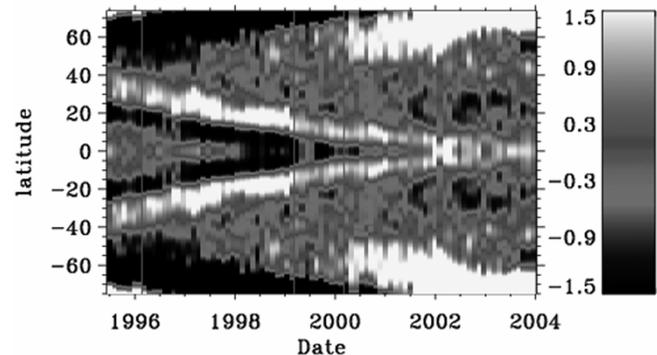

Fig. 1. Rotation residuals at a depth of 0.99 R as a function of date and latitude from an inversion of GONG data. The torsional oscillation pattern is clearly seen, and can be traced down to the middle of the convection zone. Figure courtesy of R. Howe.

Other examples of solar cycle variations obtained from global helioseismology include changes in the amplitude and lifetime of the modes (Komm, Howe and Hill, 2002), frequencies (Howe, Komm and Hill, 1999), and the rotation rate at the base of the convection zone (Howe et al., 2000). However, since solar activity occurs in regions that are much smaller than the entire sun, global helioseismology cannot be

used for space weather predictions. On the other hand, local helioseismology can provide relevant information.

3. Local helioseismology methods

Local helioseismology treats the oscillations as running waves and represents them as plane waves or rays. The conditions in the solar interior can be determined in localized areas, providing results as a function of longitude, latitude and depth, and without symmetry constraints. Thus, the conditions below active regions can be probed with local helioseismology.

There are three local helioseismology methods currently being used for space weather related studies. These are ring diagrams, time-distance, and acoustic holography.

Ring diagrams

Ring diagrams (Hill, 1988) are constructed from three-dimensional power spectra of the solar surface Doppler velocity in a localized region. The size of the region generally ranges from 2° to 30° in heliographic radius; a value of 15° is frequently used. The data in the region is projected onto a plane to allow a plane-wave approximation of the waves, and a 3-D FFT of a time series of remapped images is created. The resulting power spectrum is then cut at a constant frequency to create a ring diagram (Fig. 2).
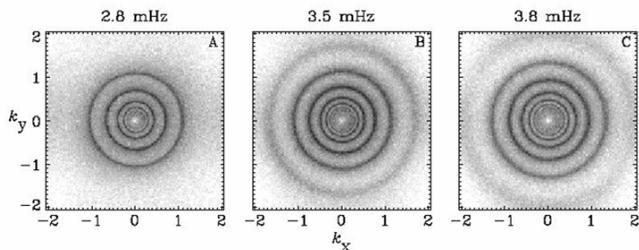

Fig. 2. Ring diagrams at three frequencies. Each ring corresponds to oscillations with different values of n, the number of radial nodes. The centroid of the rings as a function of horizontal wave number components k_x and k_y is a measure of the horizontal flow below the area in which the rings were constructed. Figure courtesy of D. Haber.

The location of each ring as a function of frequency and horizontal wave number components k_x and k_y is a depth-weighted average of the horizontal flow below the area in which the rings were constructed. The weighting functions, called kernels, are computed from theoretical solar models. The horizontal flows as a function of depth are inferred using inverse theory, and a map of the velocity field as a function of depth, altitude and longitude is constructed. The vertical velocity residual is computed from the continuity equation assuming incompressibility and using the density from a solar model. Derived fluid dynamic quantities, such as divergence, vorticity, and helicity, are computed and various averages are constructed to create maps of the flow characteristics.

Time-distance

The time-distance method (Duvall et al., 1993) is similar to one of the methods used for terrestrial seismology. Acoustic waves are emitted from a source at a specific solar location and at a certain time. The oscillations follow ray paths constrained by the solar structure, and emerge at the surface at some later time and at some distance away from the source (Fig. 3). The travel time needed to cover a distance is influenced by the conditions of the solar plasma that the wave is propagating through.
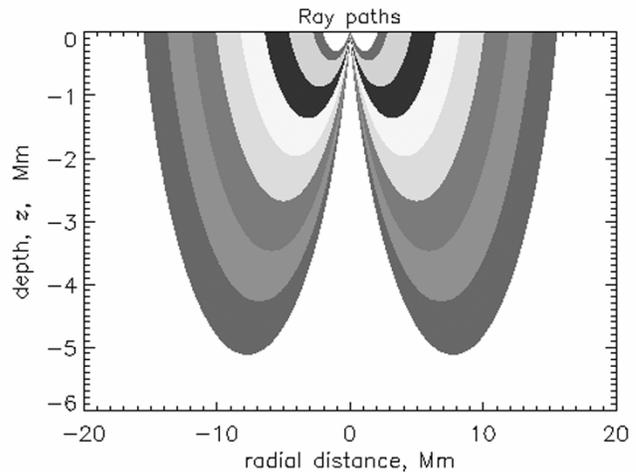

Fig. 3. Ray paths of acoustic waves emitted by a source at the surface of the sun. Figure courtesy of T. Duvall.

The construction of a time-distance diagram is conceptually simple, but computationally expensive. The first step is to compute the cross-correlation at a given time T between a point and annuli centered on the point with different radii D. This is repeated for many values of T, and an image of the cross-correlation amplitude as a function of T and D is constructed. This image is the T-D diagram, and it can also be approximately constructed by computing the Fourier transform of a phase-speed filtered oscillation power spectrum. An example of a T-D diagram is shown in Fig. 4.

The cross-correlation function can be described by a Gabor function, as shown in Fig. 4. Fitting a Gabor function to the data provides a travel time, amplitude, phase and two measurements of frequency from the envelope and oscillatory components. The travel times for many different locations are constructed, and any differences in the travel times between different points are ascribed to differences in the properties of the plasma along the ray paths. These travel time differences can be inverted to construct three-dimensional images of variations in sound speed and flow velocity (Kosovichev, Duvall and Scherrer, 2000). The time-distance method can give higher resolution images of subsurface solar structure than the ring diagrams, but the sensitivity of the method to solar structure is more complicated and the results can be hard to interpret.
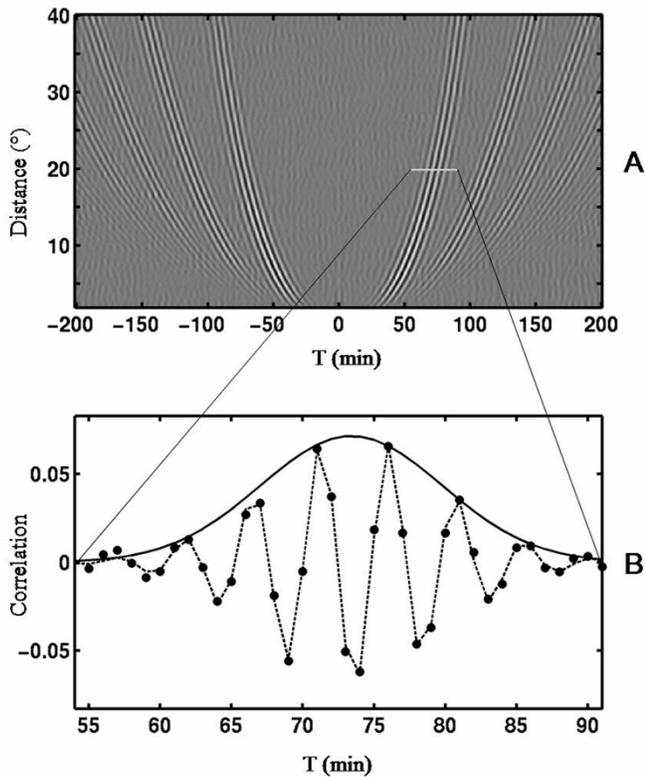
Fig. 4. Panel A: A time-distance (*T-D*) diagram showing the cross correlation of the oscillations as a function of time and distance. The different sets of ridges correspond to different numbers of reflections from the solar surface. A total of four skips can be seen. Panel B: A slice across one of the cross-correlation functions. The data is represented well by a Gabor function. The envelope of this function is shown as the solid line. Figure courtesy of O. Burtseva.

Fig. 5. Panel A: Acoustic radiation is created by the scattering of waves from features located within the sun. The radiation propagates outward and the surface disturbance is observed at the surface. This is the egression. Panel B: The observed wave field is time-reversed mathematically using a solar model down to a focal plane. This is the ingression, and it provides an acoustic image of the source shown at the bottom of the panel. The image of another source at a deeper depth is out of focus; lowering the focal plane will bring it into focus. Figure courtesy D. Braun and C. Lindsey.

Acoustic Holography

Acoustic holography (Lindsey and Braun, 2000) treats the wave field in a manner analogous to optical holography. The observed velocity field in an area (called the pupil) is regarded as the interference pattern of the background acoustic waves and waves that have been scattered from a subsurface source feature. The observed acoustic radiation emerging from the source, termed the egression, can be time-reversed mathematically with a solar model to create the ingression. The ingression will come into focus at a selected depth and provides an acoustic image of the sources at that depth. The depth can be moved to bring sources at different layers in and out of focus by filtering the waves used in the analysis. Fig. 5 shows a schematic of the process.

The source depth can be anywhere in the sun. In particular, the focus can be placed at a depth of twice the solar radius, providing images of the far side of the sun (Braun and Lindsey, 2001). Fig. 6 shows how this is done. In this case the waves that are used have much larger spatial wavelengths than is usually the case in local helioseismology. The pupils are correspondingly large, and are rotated across the visible disk in order to change the spatial location of the farside focus.
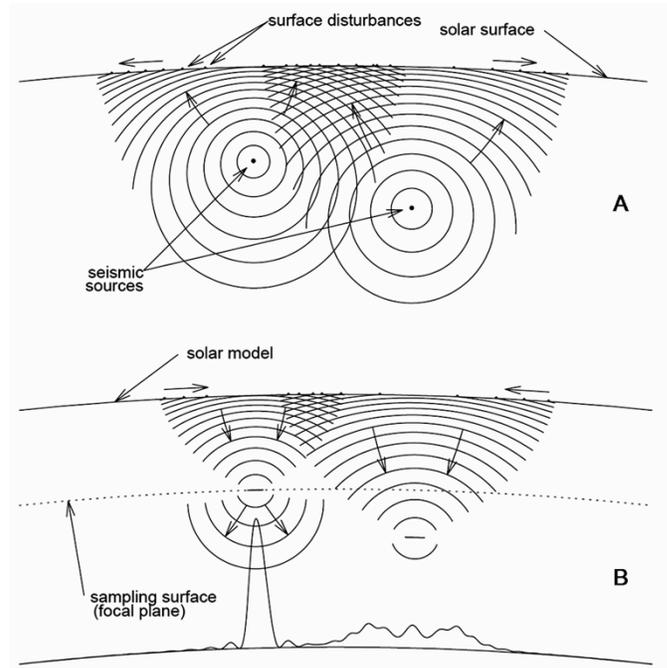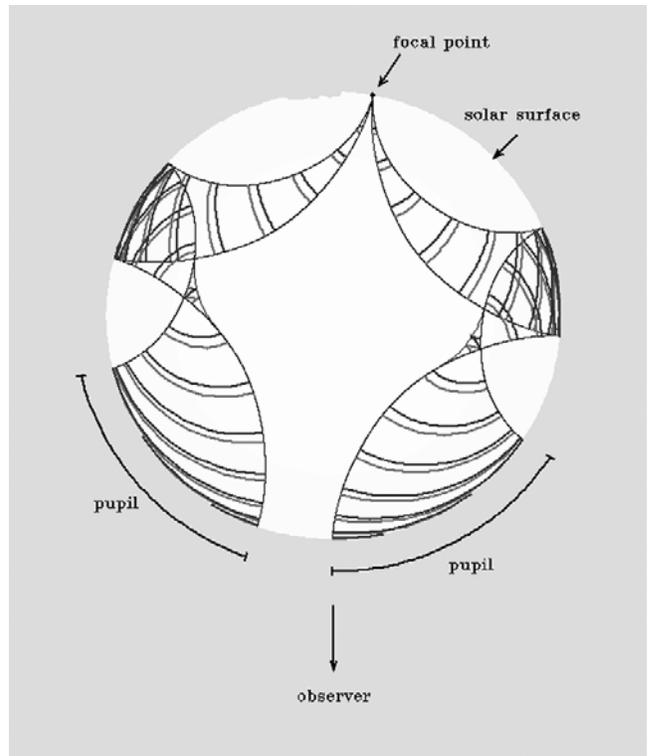

Fig. 6. Farside imaging using acoustic holography. Waves with large spatial wavelengths are used to place the focal plane on the farside. The pupils on the front side are rotated across the disk to change the spatial location of the farside focus. Figure courtesy D. Braun and C. Lindsey.

4. Results

This section summarizes some relevant results for space weather prediction.

Subsurface flows and flare activity

Using ring diagrams, Komm et al. (2004) found that a velocity field with strong zonal vorticity was present below AR10486, the source of the strong Halloween flares. This flow field is shown in Fig. 7.
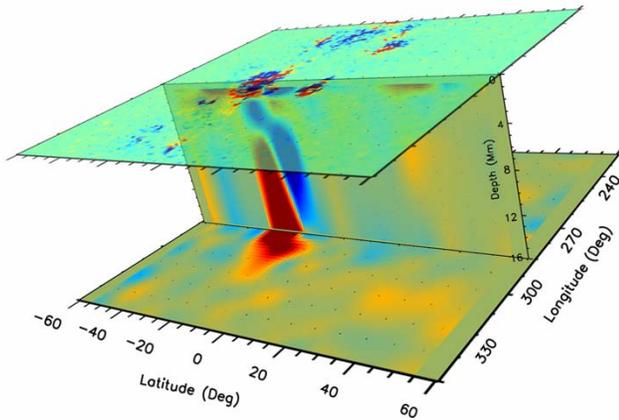

Fig. 7. The subsurface flows below AR10486, the source of the October-November 2003 "Halloween" flares. The surface magnetogram is shown in the plane at the top of the image, while the flow is visible as the red and blue structure. The colors show the two senses of the zonal vorticity below the active region. Figure courtesy of R. Komm

Mason et al. (2006) studied the statistical relationship between the subsurface vorticity derived from ring diagrams and the flaring activity of active regions. Using 408 active regions observed by MDI and GONG, they found that there is a strong correlation between a specific pattern of subsurface vorticity, the strength of the magnetic field, and the strength of flare activity at the surface. This indicates that two conditions must be present for flare activity in an active region: a strong magnetic field, and a flow with sufficient rotational energy to twist the field into an unstable configuration.

The temporal behavior of the subsurface flows may provide a way to predict flare activity on the time scale of a few days (Komm et al., 2004). Fig. 8 shows the temporal behavior of the kinetic helicity obtained from ring digrams in the vicinity of AR10486. In the two analysis areas where the active region was located, the value of kinetic helicity was substantially larger prior to the flare than in the adjacent areas. In addition, the helicity signal decreased back to quiet sun levels at the time of the flare.

Ambastha, et al. (2004) also used ring diagrams to study flows below flaring regions. They found a steeper gradient of meridional (north-south) flow and an absence of the near-surface zonal (east-west) shear layer in areas with high flare activity.
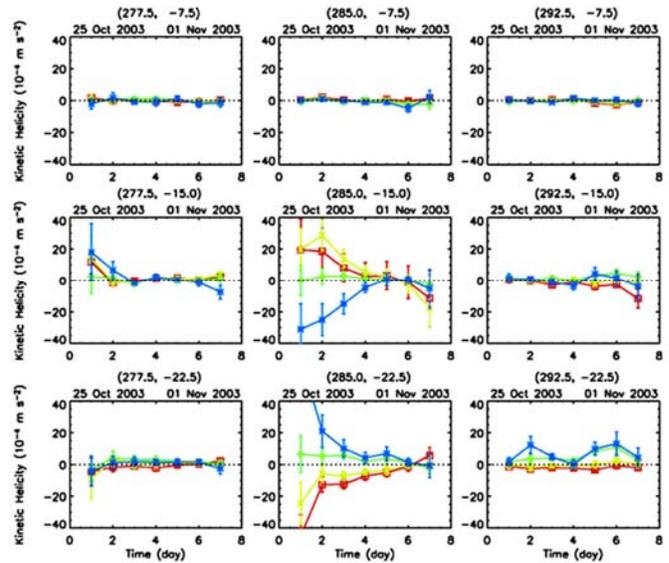

Fig. 8. The subsurface kinetic helicty as a function of time in nine areas in the vicinity of AR10486, which is divided between the central area and the area immediately below. The different curves are for different depths. A strongly enhanced signal is seen at the location of and temporally before the flare; this signal is seen to return to quiet sun levels after the occurrence of the flare on October 29 (day 5). Figure courtesy of R. Komm

Emerging active regions

The time-distance method has been used to determine the differences in travel time due to sunspots, as seen in Fig. 9, which shows that the travel time is decreased in regions of higher activity. This decrease is due to an increase of the sound speed below the sunspot presumably from a combination of higher temperatures and stronger magnetic fields.
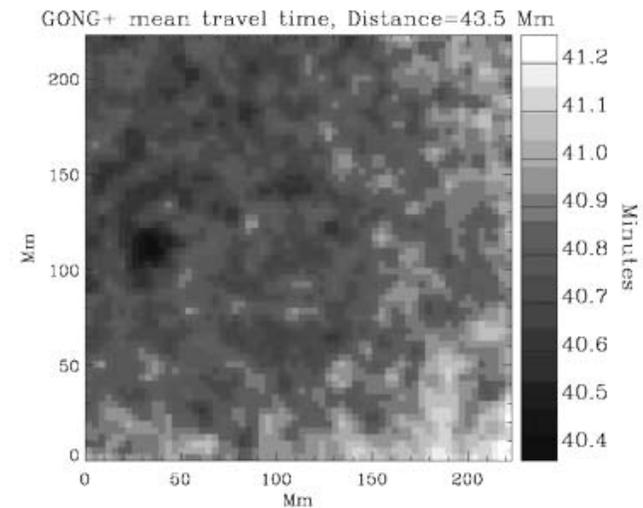

Fig. 9. A grey scale map of the travel time for acoustic waves for a distance of 43.5 Mm. A sunspot is located near the position (50, 100) where the travel time is decreased due to higher temperatures and stronger magnetic fields below the active region. Figure courtesy of P. Rajaguru.

Inversions of the travel time differences have been used to detect an active region rising through the outer convection

zone before it appears at the surface. This is shown in Fig. 10, which displays a series of sound speed images of AR10488 as it emerged at the surface. This sequence illustrates that time-distance helioseismology could predict the existence of an active region a few days before it appears in the photosphere.
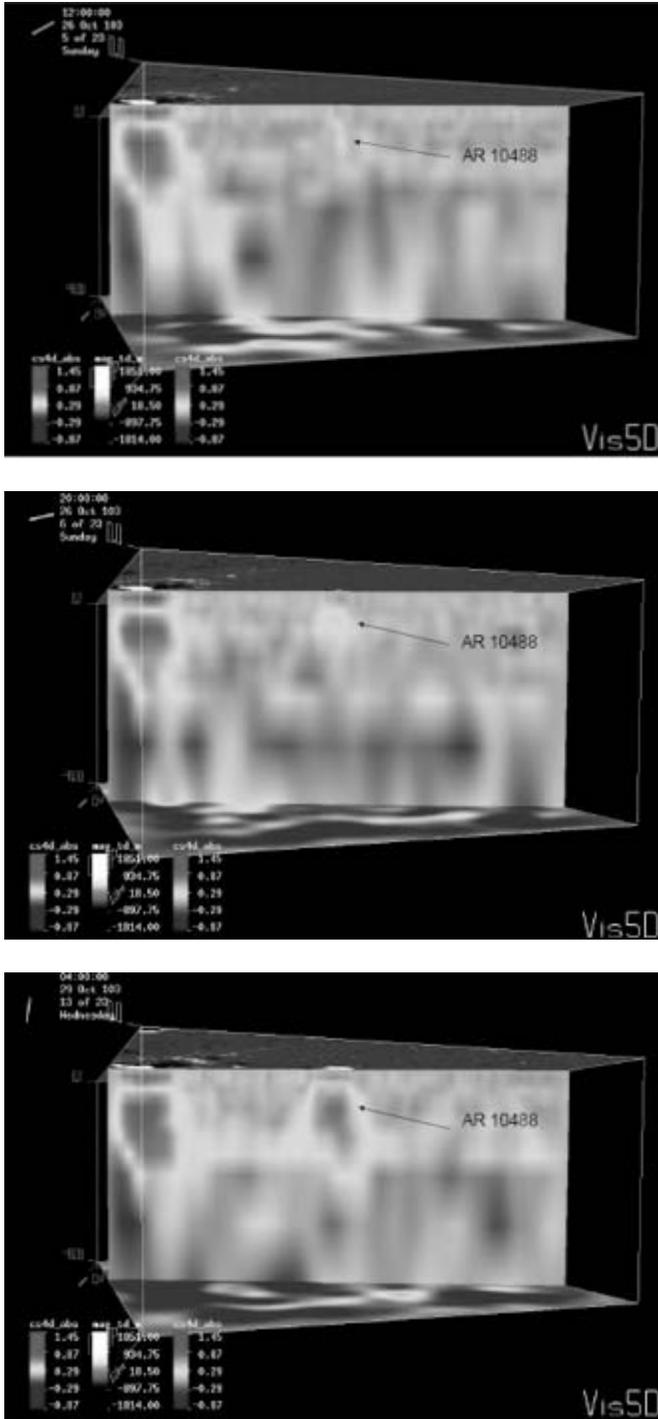

Fig. 10. A sequence of time-distance inversions showing the emergence of AR10488. Top: Oct. 26, 2003 12:00 UT. Center: Oct. 26, 2003 20:00 UT. Bottom: Oct. 29, 04:00 UT. The grey scale shows relative sound speed fluctuations. The temporal evolution of the sound speed fluctuations as AR10488 emerges is clearly seen. Figure courtesy of T. Duvall and A. Kosovichev.

Detection of active regions on solar farside

Acoustic holography is capable of detecting large active regions on the farside of the sun thereby providing an early warning of potential flares up to 14 days in advance. This is illustrated in Fig. 11, which shows a time sequence of farside maps containing AR10808 in early September 2005. On Sept. 7, the Solar X-Ray imager on the GOES satellite detected a large X-17 flare. This occurred in AR10808 as it appeared on the eastern limb.
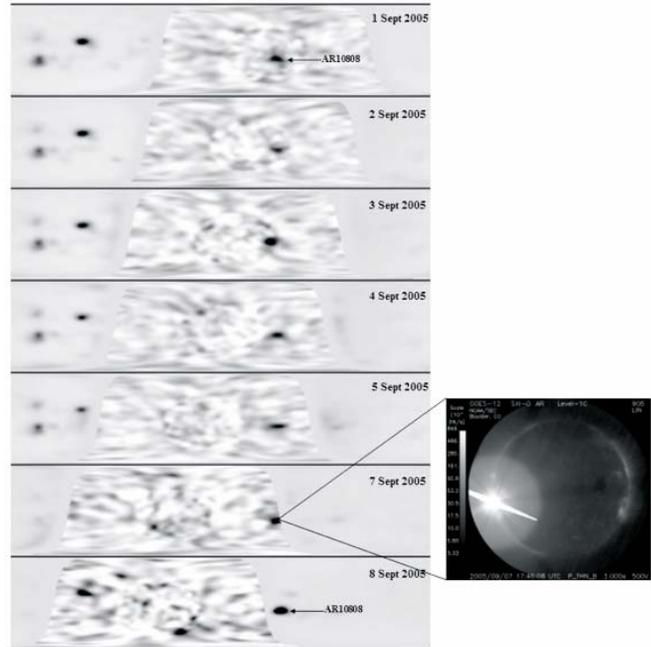

Fig. 11. Left: A sequence of farside maps derived from GONG observations covering the period of 1 Sep. to 8 Sep. 2005. A strong persistent feature is visible, and was subsequently identified as AR10808. Right: An X-17 flare occurred in AR10808 on Sep. 7, 2005 as it moved onto the visible disk. Figure courtesy of I. González-Hernández and C. Lindsey.

In order to develop farside imaging into a useful tool for predicting solar activity, it is essential to derive a calibration between the observed phase shift in the farside map, and the strength of the magnetic field. This is not a simple task, since it is not possible to obtain magnetic field measurements at the same time and location of the farside signal. A bootstrap method will have to be used to construct an empirical relationship.

5. Summary and discussion

The techniques of local helioseismology are now beginning to provide predictions of solar activity that will contribute to the development of space weather forecasting. The ring diagram method is demonstrating that specific flow configurations are likely activity producers and that there may be precursor temporal variations that can be used as predictors. Time distance methods allow us to see large active regions forming below the surface on the disk, giving a one to five day warning before they appear in the photosphere. The technique of acoustic holography can detect very large active regions on the solar farside, giving up

to a 14-day warning before their appearance on disk, or an all-clear signal for a similar period.

There are, however, a number of issues that need to be resolved before local helioseismology can be reliably used as a tool for space weather forecasts. Some of these issues are:

- The establishment of confidence levels – predictive tools must be able to place a quantitative confidence level on the forecast, i.e. a 75% change of a flare in a given active region. In addition, false alarm rates must be estimated. This requires statistical studies of the predictions.
- Better understanding of the effect of spectral line profile changes on the results – recent work (i.e. Rajaguru, Wachter and Hasan, 2006; Edelman et al., 2004) suggests that changes to the profile of the spectral line used in the observations could influence the results.
- Better understanding of flare-related flow characteristics – models of the flow and magnetic field and their interaction are essential for understanding the observations.
- Tighter connection with surface observations – what is the relation between the flow and the surface neutral line?
- Incorporation of the subsurface flows into coronal mass ejection (CME) and flare initiation models.
- Energy analysis – velocity vs magnetic field, is there a CME or a solar energetic particle event associated with a particular flow pattern?
- Faster data delivery and analysis – while the farside method can give results in a few hours, other methods can take days to perform. This is not useful for predictions.
- Calibration of the farside signal in terms of magnetic field strength and activity levels. This is needed to make the farside signal a more useful predictive tool.
- A comparison of subsurface flows and the direction of the magnetic field – new vector magnetograms will soon be available from SOLIS and HMI. It will be of interest to compare the subsurface flows and the directions of the field.

With further development, we can expect that local helioseismology will make a substantial contribution to the prediction of space weather.

References

A. Ambastha, S. Basu, H. M. Antia and R. S. Bogart, "Solar p-mode characteristics associated with superactive regions observed during Oct Nov 2003", in *Helio- and Asteroseismology: Towards a Golden Future,* D. Danesy, Ed. Noordwijk: ESA SP-559, 2004, pp. 293-296.

D. C. Braun and C. Lindsey, "Seismic imaging of the far hemisphere of the sun", *Astrophys. J.,* vol. 560, pp. L189-L192, 2001.

T. L. Duvall Jr., S. M. Jefferies, J. W. Harvey and M. A. Pomerantz, "Time-distance helioseismology", *Nature*, vol. 362, pp. 430-432, 1993.

F. Edelman, F. Hill, R. Howe and R. Komm, "The effect of spectral line shape changes on GONG observations of oscillations and flares", in *Helio- and Asteroseismology: Towards a Golden Future,* D. Danesy, Ed. Noordwijk: ESA SP-559, 2004, pp. 416-419.

F. Hill, "Rings and trumpets: three-dimensional power spectra of solar oscillations", *Astrophys. J.,* vol. 333, pp. 996-1013, 1988.

R. Howe, J. Christensen-Dalsgaard, F. Hill, R. Komm, R. M. Larsen, J. Schou, M. J. Thompson and J. Toomre, "Dynamic variations at the base of the solar convection zone", *Science,* vol. 287, pp. 2456-2460, 2000.

R. Howe, J. Christensen-Dalsgaard, F. Hill, R. Komm, J. Schou and M. J. Thompson, "Solar convection-zone dynamics, 1995-2004", *Astrophys. J.,* vol. 634, pp. 1405-1415, 2005.

R. Howe, R. Komm and F. Hill, "Solar-cycle changes in GONG p-mode frequencies 1995-98", *Astrophys. J.*, vol. 524, pp. 1084-1095, 1999.

R. Komm, R. Howe, I. González Hernández, F. Hill, J. Sudol and C. Toner, "Searching for subsurface signatures of X-class flares", in *Helio- and Asteroseismology: Towards a Golden Future,* D. Danesy, Ed. Noordwijk: ESA SP-559, 2004, pp. 158-163.

R. Komm, R. Howe and F. Hill, "Localizing width and energy of solar global p modes", *Astrophys. J.*, vol. 572, pp. 663-673, 2002.

A. G. Kosovichev, T. L. Duvall Jr. and P. H. Scherrer, "Time-distance inversion methods and results", *Solar Phys*. vol. 192, pp. 159-176, 2000.

C. Lindsey and D. C. Braun, "Basic principles of solar acoustic holography", *Solar Phys*. vol. 192, pp. 261-284, 2000.

D. Mason, R. Komm, F. Hill, R. Howe, D. A. Haber and B. W. Hindman, "Flares, magnetic fields, and subsurface vorticity: A survey of GONG and MDI data", *Astrophys. J.*, vol. 645, pp. 1543-1553, 2006.

S. P. Rajaguru, R. Wachter and S. S. Hasan, "Influence of magnetic field on the Doppler measurements of velocity field in the solar photosphere and implications for helioseismology", in these proceedings, 2006.

H. C. Spruit, "Origin of the torsional oscillation pattern of solar rotation", *Solar Phys*., vol. 213, pp. 1-21, 2003.